electronics

Communication

Stochastic Geometry-Based Analysis of Heterogeneous Wireless Network Spectral, Energy and Deployment Efficiency

Jasmin Musovic [1], Vlatko Lipovac [2] and Adriana Lipovac [2,*]

[1] Communications Regulatory Agency, 71000 Sarajevo, Bosnia and Herzegovina; jmusovic@rak.ba
[2] Deparetmet of Electrical Engineering and Computing, University of Dubrovnik, 20000 Dubrovnik, Croatia; vlatko.lipovac@unidu.hr
* Correspondence: adriana.lipovac@unidu.hr; Tel.: +385-20445734

Abstract: For quite a while, it has been evident that homogeneous network architectures, based on cells with a uniform radiation pattern, cannot fulfill the ever increasing demand of mobile users for capacity and service quality while still preserving spectrum and energy. However, only with the introduction of the Fourth Generation mobile communication networks to deal with the surging data traffic of multimedia applications, have smaller cells been widely used to break down service zone areas of macro base stations into multiple tiers, thus improving network performance, reducing traffic congestion, and enabling better management of spectrum and energy consumption in a macro network. In this paper, we present an analytical model for assessing the efficiency of bandwidth and energy usage, as well as of network deployment, taking into account overall network investment and maintenance costs. This paves the way to the improved planning of network coverage, and its capacity and reliability, thus preserving its spectrum and energy, as well as the environment. The analysis considers the downlink of an arbitrary heterogeneous cellular network by using tools of stochastic geometry that adopt the distribution of base stations in the form of a Poisson Point Process. The proposed analytical model is verified by the according software simulations using the ns-3 network simulator. The obtained results closely match the theoretically predicted values and boundaries, clearly indicating that, in all three analyzed aspects: spectral, energy, and deploymental, the efficiency of small-cell networks was higher with respect to traditional large-cell networks and increased even further for heterogeneous (two-tier in our tests) networks.

Keywords: heterogeneous cellular network; spectral efficiency; deployment efficiency; Poisson Point Process; ns-3

check for updates

Citation: Musovic, J.; Lipovac, V.; Lipovac, A. Stochastic Geometry-Based Analysis of Heterogeneous Wireless Network Spectral, Energy and Deployment Efficiency. *Electronics* **2021**, *10*, 786. https://doi.org/10.3390/electronics10070786

Academic Editor: Francisco Falcone

Received: 9 February 2021
Accepted: 22 March 2021
Published: 26 March 2021

1. Introduction

With the deployment of the Third Generation (3G) wireless systems, it became evident that homogeneous network architectures, based on cells with uniform radiation pattern in service zones, could not fulfill the ever increasing demand of mobile users for capacity, service quality, and economically efficient energy consumption. This evidence has become even more pronounced with the introduction of the Fourth Generation (4G) networks, when implementing smaller cells has become a way to improve network performance, reducing traffic congestion in macro networks. Hence, for example, plug-and-play installation of femto-cells is much simpler and more profitable than whatever can be achieved with macro cells, due to reduced backhaul costs. The smaller the cell, the less power needs to be transmitted, so small cells can serve small groups of users (UE), and thus can improve the quality of service (QoS) [1].

Furthermore, complex Radio Access Systems (RAS) can comprise cells of various classes, thus forming the so-called Heterogeneous Cellular Network (HCN), also commonly referred to as HetNet, where the basic topology concept presumes layering two or more groups of the same-class cells, called tiers [2,3].

Over the last decade, the rapid evolution of mobile telecommunication services fueled by growing demand for multimedia applications has led to surging data transmission traffic, which (according to annual reports of major network operators and network equipment manufacturers) increases approximately ten times every five years, to reach about 12 Exabytes per month—13 times more than in 2017.

The very direct consequence of such data traffic growth is the increasing demand for RAS nodes, which severely affects energy efficiency. Hence, for example, the average annual energy consumption of a single base station (BS) is about 25 MWh [4], which significantly contributes to almost 2% of the global carbon emission currently estimated to be generated by ICT industry.

Although HetNet cell planning has been in use even in the Second Generation (2G) mobile networks, it is only the Long Term Evolution (LTE) and its extension LTE Advanced (LTE-A), commonly referred to as 4G standard, which fully define the concept for enhancing the HetNet performance.

Such strategies for LTE/LTE-A radio performance planning are centered around reducing the distance between the transmitter and receiver, i.e., improving the service signal coverage of regions demanding more intensive traffic. Accordingly, in Figure 1, examples of a simplified HetNet with a multistandard 4-tier scenario (a), and 3-tier topology (b), are presented.

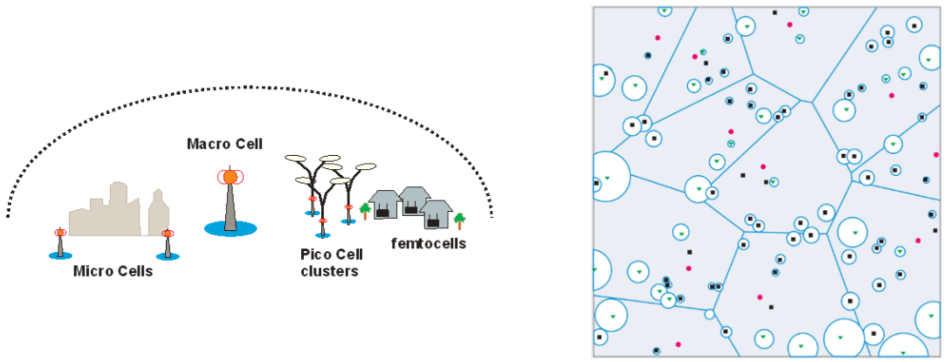

(**a**) (**b**)

Figure 1. Simplified presentations of an exemplar Heterogeneous Cellular Network (HCN), also commonly referred to as HetNet, (HetNet¬); (**a**) multiple-standard radio access HetNet; (**b**) 3-tier HetNet coverage with blue lines as service zones' boundaries, and red spots, green triangles, and black squares as macro-cells, pico-cells, and femto-cells, respectively.

We investigate network energy efficiency according to the following metrics proposed for wireless access networks [5,6]:

- energy per information bit [J/b];
- average power used by a device that provides connectivity to a certain covered area [Wm^2].

Beside service provisioning, the European Telecommunications Standards Institute (ETSI) proposes the following QoS-related metrics [7]:

- ratio between the throughput of users obtaining the minimal specified (service dependent) QoS within the served area, and the total power consumed by the BSs providing service in that area [b/J];
- ratio between the number of UEs obtaining the minimal specified QoS within the served area, and the total energy consumed by the BSs providing service in that area during the observation time.

The essence of the proposed metrics is improving HetNet coverage and capacity, both dependent on signal-to-interference-plus-noise-ratio (SINR).

Therefore, we investigate various scenarios in HetNets and SINR values that might occur at the receiver of each UE [8] within the area of the serving tier, served by a single BS, and a single candidate-serving BS. The SINR analysis points to the network spectral efficiency (SE) and deployment efficiency (DE).

Basically, two approaches have been used in the analysis of large networks:

- hexagonal grid-based, which assumes that the cellular network is composed of a grid of hexagons representing cells with a BS placed in the center of each cell [9,10];
- stochastic geometry-based, which not only captures the topological randomness in the network geometry but also enables tractable and accurate analysis [9,11,12].

The HetNet topology structure can be presented in the form of Poisson Point Process (PPP) [8], as the BSs are stationary within a network area. Such a model can well describe irregular placements of BSs within a real network, rather than the traditional hexagonal model [9]. The topology analysis in the PPP form dates back to quite a while ago [10,11,13], but only recently have the network coverage and capacity been modeled as PPP [9] and the PPP-distributed BSs applied to various network scenarios including heterogeneous mobile networks [12,14–17], MIMO mobile networks [18,19], and MIMO HetNets [20,21].

The contributions of this work can be summarized as it follows:

(1) We characterize the distribution of BSs in a certain network area, where the locations of BSs and UEs are considered to be PPPs. We consider the UEs from open-access (OA) small cells, and not the ones belonging to closed subscriber groups (CSG). In addition, the serving BS is selected on the basis of the cell range extension (CRE), and the analytical expressions for EE and SE are derived for the two scenarios of interest.

(2) We introduce the joint analysis of SE, EE, and cost-oriented DE. This holistic approach has already been applied [22], but in this investigation, we enhance the model to exhibit the trade-offs among the three parameters.

(3) Finally, the simulation results validate the benefits of cell planning according to the proposed model and recommended simulation configuration set-up [23]. It is possible to further improve the analysis by involving complexity and fairness, if the model is enhanced by various mechanisms of network resources' management [24].

In Section 2, we first review some basic theories and the trade-off between spectral and energy efficiency in terms of theoretical transmission performance boundaries.

Then, we present the stochastic geometry-based model for the analysis of large HetNets with randomly distributed candidate-serving and serving BSs within the serving-tier area, while taking into consideration three major issues: SINR, SE, and DE.

Furthermore, to validate the analytical model, in Section 3, we report the results of the simulation conducted by means of ns-3 tool to get the instantaneous SINR values at each UE receiver of the network under test. In Section 4, discussion of the obtained results is provided, whereas the conclusions are drawn in Section 5.

2. Analysis

In multiuser real-life radio networks, the relationship between the spectral efficiency (*SE*) and the energy efficiency (*EE*) is determined by compromises among the network throughput $\overline{T_{TOT}}$, the total system energy $\overline{E_{TOT}}$, distribution of frequency resources, traffic flows, minimal probability of erroneous data units, and QoS.

2.1. Basic Theory and EE vs. SE Relationship

Specifically, *SE* is a performance measure of wireless communication systems, which presents transmission rate R [b/s] achievable for given bandwidth B [Hz], i.e., *SE* is expressed as the ratio R/B.

On the other hand, the radio channel *EE* [b/J] is described as the dimensionless ratio E_b/N_0 between the energy per bit and the noise spectral density, which is in fact the count of the transmitted information bits per energy unit.

Hence, as the two very basic resources of a radio channel—bandwidth B and mean power P_S—determine its Shannon capacity C, we can express the latter by SE and EE as follows:

$$C = B \cdot log_2\left(1 + \frac{P_s}{P_N}\right) = B \cdot log_2\left(1 + \frac{E_b}{N_0} \cdot \frac{R}{B}\right) = B \cdot log_2(1 + SE \cdot EE) \tag{1}$$

Specifically, in case of a Additive-White-Gaussian-Noise (AWGN) channel, it is well known that for given P_S and B, EE can be expressed as the ratio of C and B, which applied to (1) implies that:

$$SE = \log_2(1 + SE \cdot EE) \tag{2}$$

Hence, the explicit relationship between EE and SE is:

$$EE = \frac{2^{SE} - 1}{SE} \tag{3}$$

Applying (3) to the simplest wireless network consisting of a single BS and a single UE, we can analyze relations in various power and energy regions of the channel, which are determined by a SE and EE relationship, with the goal of enabling a significantly larger throughput and data rate.

In this regard, let us consider two exemplar cases, which are characteristic for the linear and the non-linear region of the EE vs. SE relationship.

In the first case, let us assume the spectral efficiency as low as SE = 0.1 b/s/Hz. In order to increase the throughput eight times, the received signal power needs to be increased about ten times. This example reflects the almost linear relationship between the increment of the information data rate and the required power at the receiver frontend, which, however, is not applicable to demanding services requiring higher data rates, Figure 2.

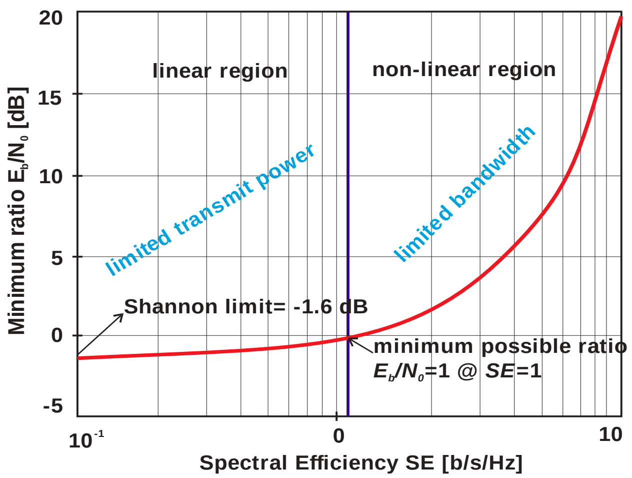

Figure 2. Spectral efficiency (SE) and energy efficiency (EE) (Eb/N0) relationship.

Nevertheless, for higher SE in the order of 2 b/s/Hz, to increase the data rate only four times while keeping the same bandwidth, the received signal power needs to be increased about 85 times, whereas to increase the data rate ten times, the necessary received signal power must ramp up about 300,000 times, Figure 2.

From these examples, it is obvious that the increasing data rate requires a significant increase of the received signal power.

This implies reducing distances between BS and UE down to tens of meters, whereas the linear-region models tolerate considerably longer distances, but with significantly lower SE, as a consequence of reducing EE, due to channel propagation effects.

However, if the above identified problem is considered at a network level with multiple UEs using the selected multiple access scheme, very complex processes can arise, where *EE* plays a dominant role:

- In linear-region models, such as is the case with 2G mobile networks, *EE* significantly decreases towards the cell edge, which also implies the reduction of *SE* and therefore also of the throughput. A particular negative aspect of such models is the almost uniform distribution of the signal energy across the cell, as equal coverage of areas with few active UEs is definitely not a rational use of energy resources. Hence, e.g., reducing the cell radius from 1000 m to 250 m results in *EE* increasing from 0.11 Mb/s/J to 1.92 Mb/s/J (for a 3G system), which is equivalent to increasing *EE* 17.5 times [25].
- Moreover, the models with huge cell dimensions require large BS power, which is not welcome in zones around the BS, due to high electromagnetic radiation density and its potentially dangerous impact in highly populated areas.
- In non-linear-region models, significantly better *EE* is achievable, as stronger received signals inevitably imply the significant reduction of cell dimensions down to tens of meters, giving rise to various cell classes in this regard: micro, nano, pico, and femto, which ensure:
    - closer-to-uniform *EE* distribution,
    - significantly higher *SE* and so the throughput alike,
    - rational coverage with satisfactory *EE*, especially in the areas of many active users, and
    - significantly reduced EM radiation density.

2.2. Analytical Model

The PPP models for representing BS deployment are widely accepted for various HetNet scenarios. While hexagonal models do not well represent real networks, the PPP ones are much more appropriate for this purpose [26]. Actually, among the PPP variants, such as the Matérn Hard-Core Process (MHCP) [27], the one with non-uniformly distributed BSs is most often used. It is important to note that the PPP distribution of locations determines the SINR values for each user, i.e., that SINR depends on the UE-BS distance. This is sufficient for the analysis, as the other PPP variants consider the minimization of locations' distances, which matters in academic terms, but for real networks, increases the analysis complexity to the extent of becoming a problem in other scenarios that are themselves complex, especially in 5G networks.

Thus, the overall HetNet efficiency has been analyzed through joint analysis of SE and DE by assessing SINR at an arbitrary UE, and considering network topology as a stochastic geometry form.

Hence, we observe the signal at the receiver of an arbitrary end-user UE located in a k-tier heterogenous cellular network consisting of N_T tiers overall.

Moreover, it is quite justifiable to assume that the signal-to-noise ratio (*SNR*) is high, and that the (RF) interference from other radio signal sources is a dominant impairment.

Each tier is considered to be a homogeneous PPP Φ_k, characterized by triplet (P_k, λ_k, τ_k) which denotes:

- total transmit power in each tier,
- density of BSs and
- SINR threshold τ (below defined as bias) at UE to restore data, respectively.

The tiers are ranked in ascending order by the density of access points, i.e., $\lambda_1 \leq \lambda_2 ... \lambda_{k-1} \leq \lambda_k$. Given the density λ_k, the number of access points belonging to tier k_i (i = 1,2, ... ,N_T) in the network area $\mathcal{A}$ [m^2] represents a random Poisson variable, with the mean density $\mathcal{A} \cdot \lambda_k$, which is independent of other tiers. Furthermore, all access points in the k-tier have the same transmission power P_k.

Each downlink is modeled by the Rayleigh fading channel, where P_i^{tx} and P_i^{rx} are the transmitted (from BS) and the received power (at an arbitrary UE$_i$ at R_i distance from BS), respectively.

The model considers the path-loss exponent to be equal to 4 [2]. There are n_{ABS} Almost Blank Subframes (ABS) in which macro BSs do not transmit any power [3].

For each tier, the factor of frequency reuse equals 1, and the RF band is allocated in a way that one real channel is skipped between two tiers of the same wireless technology standard. Thus, for a typical UE connected to tier k, the set of interfering BSs include all BSs in tier k except the serving one.

We assumed the scenario where the user is only allowed to access the BSs in tiers 1,2,...,K_{open} which belong to macro/pico cells with Open Access (OA), whereas the Closed Subscriber Group (CSG) femtocells are not allowed to serve the users under consideration, which is the most common case [8]. For example, HetNet would be represented by the count of tiers: N_T = 3 and the count of tiers with OA: N_{open} = 2, with tier 1 representing the macro cells, tier 2 the OA pico cells, and tier 3 the CSG femtocells.

Furthermore, we assume that each BS in the observed tier transmits with maximal power allowed for BSs in that tier (We do not analyze here the scenario where the user moves quickly through service zones of two and more BSs, so initiating handoffs [28]).

To demonstrate the relationship between DE and SE, it is necessary to firstly analyze the relationship between the network SE and the total power in such a way that the base stations are distributed within the tiers in the form of PPP.

The BS b_k of any serving tier k_i transmits only to a specific subset of the users U_b served by $b_k \in \Phi_k$. Let us denote $\Gamma(u_b)$ as the SINR at the specific user $u_b \in U_b$.

The spectral efficiency SE_k of the link from b_k to the randomly chosen target u_b is:

$$\begin{gathered} SE_b \equiv E\{log_2[1+\Gamma(U_b)]\} \\ b \in \Phi,\ P\{U_b = u_b\} = \frac{1}{|U_b|}, u_b \in U_b \end{gathered} \tag{4}$$

2.2.1. Network Spectral Efficiency

The proposed analytical model considers the spectral efficiency SE_k for each tier ($k = 1 \ldots N_T$), as well as SE_{TOT} for the whole HetNet.

The technique for selecting serving or candidate-serving cells in the LTE-A standard is, among other factors, based on the cell range extension (CRE), which has been proposed for pico-cell BSs to enable traffic load balancing and to prevent inter-cell RF interference in the areas of overlapping coverage.

In this regard, the important parameter is the range expansion bias (REB), taking the values of τ within the range θ. It is applied to the mean received pilot powers at the UE, coming from the candidate-serving macro and pico BSs to make the optimal selection of the small-cell tier to serve the UE according to two scenarios described in the following:

In the first case, macro tier i is the serving tier, while pico tier j is the candidate-serving tier, whereas in the second case, the UE is served by pico tier j, while having macro tier i as the candidate-serving one [8].

The distance from the UE to the candidate-serving (i.e., the nearest) macro BS is $\mathcal{R}_i$, whereas the distance between the UE and the candidate-serving (the nearest) pico BS is $\mathcal{R}_j$.

In order to derive a simplified model of HetNet SE, we consider the instantaneous transmit power of any macro BS to be a random variable equal to either zero during the ABS state, or to P_1^{tx}, otherwise, while the instantaneous transmit power of the serving BS is denoted as P_2^{tx}.

In this way, the selection bias for tier k is:

$$\tau = \sqrt[4]{0.063 \cdot \theta \cdot \frac{P_2^{\text{tx}}}{P_{1,}^{\text{tx}}}} \tag{5}$$

In the first case, we consider an arbitrarily located UE served by micro tier i, and the probability of its SINR, herewith defined as Γ_i, to be greater than the threshold—the SINR expected value γ.

According to (1) and (2), the spectral efficiencies SE_i and SE_j of these two scenarios, respectively, can be expressed in the following form [8]:

$$\begin{aligned} \mathcal{P}_i &= \mathcal{P}\{\Gamma_i > \gamma \parallel \mathcal{R}_i = r_i, \mathcal{R}_j = r_j\} = \\ &= (1 - n_{ABS})\cdot\mathcal{P}\{\Gamma_i > \gamma \parallel \mathcal{R}_i = r_i, \mathcal{R}_j = r_j\} = \\ &= 0.75\cdot e^{-\pi\cdot\lambda_i\cdot r_i^2\cdot\sqrt{\gamma}[cot^{-1}(\frac{1}{\sqrt{\gamma}})+\beta cot^{-1}(\frac{\pi\cdot\lambda_j\cdot r_j^2}{\beta\cdot\pi\cdot\lambda_i\cdot r_i^2\cdot\sqrt{\gamma}})]} \end{aligned} \tag{6}$$

where r_i and r_j are instantaneous distances from UE to the serving macro BS and serving pico BS, respectively, whereas β is:

$$\beta = \frac{\lambda_2}{\lambda_1}\sqrt[4]{0.063\cdot\theta\cdot\frac{P_2^{\text{tx}}}{P_1^{\text{tx}}}} \tag{7}$$

For the second case, the probability that UE is served by the pico tier, having the satisfactory level of SINR, denoted as Γ_j, is as follows:

$$\begin{aligned} \mathcal{P}_j &= \mathcal{P}\{\Gamma_j > \gamma \parallel \mathcal{R}_i = r_i, \mathcal{R}_j = r_j\} = \\ &= (1 - n_{ABS})\cdot\mathcal{P}\{\Gamma_j > \gamma \parallel \mathcal{R}_i = r_i, \mathcal{R}_j = r_j\} + \\ &+ n_{ABS}\cdot\mathcal{P}\left\{\Gamma_j^{ABS} > \gamma \parallel \mathcal{R}_i = r_i, \mathcal{R}_j = r_j\right\} \\ &= 0.75\cdot e^{-\pi\cdot\lambda_i\cdot r_i^2\cdot\sqrt{\gamma}[cot^{-1}\frac{(1)}{\sqrt{\gamma}}+\beta cot^{-1}(\frac{\pi\cdot\lambda_j\cdot r_j^2}{\beta\cdot\pi\cdot\lambda_i\cdot r_i^2\cdot\sqrt{\gamma}})]} + 0.25\cdot e^{-\pi\cdot\lambda_j\cdot r_j^2\cdot\sqrt{\gamma}\cdot cot^{-1}(\frac{1}{\sqrt{\gamma}})} \end{aligned} \tag{8}$$

The probability density functions of the UE distances from serving tier i and from candidate-serving tier j are as follows:

$$f_{\mathcal{R}_i}(r_i) = 2.5\cdot\pi\cdot\lambda_i\cdot r_i\cdot e^{-1.25\cdot\pi\cdot\lambda_i\cdot r_i^2} \tag{9}$$

$$f_{\mathcal{R}_j}(r_j) = 2\cdot\pi\cdot\lambda_j\cdot r_j\cdot e^{-\pi\cdot\lambda_j\cdot r_j^2} \tag{10}$$

respectively.

Developing (9) and (10) converges to the following relations, which comprehend spectral efficiencies of the macro and pico tier, respectively, as:

$$SE_i = \frac{\lambda_i}{\ln 2}\int_0^\infty\int_0^\infty\int_{\tau\cdot r_i}^\infty \frac{f_{\mathcal{R}_i}(r_i)\cdot f_{\mathcal{R}_j}(r_j)\cdot\mathcal{P}_i}{1+\gamma}d\gamma dr_i dr_j \tag{11}$$

$$SE_j = \frac{\lambda_j}{\ln 2}\int_0^\infty\int_0^\infty\int_{\frac{r_i}{\tau}}^\infty \frac{f_{\mathcal{R}_i}(r_j)\cdot f_{\mathcal{R}_j}(r_i)\cdot\mathcal{P}_j}{1+\gamma}d\gamma dr_j dr_i \tag{12}$$

The overall HetNet spectral efficiency is:

$$SE_{\text{TOT}} = SE_i + SE_j \tag{13}$$

2.2.2. Network Deployment Efficiency Analysis

In order to estimate the 2-tier HetNet DE according to the described scenarios, we derive a simple cost-oriented power model using the data sourced from incumbent network operators in Bosnia and Herzegovina, which we broke down into capital expenditure (CAPEX), operating expenses (OPEX), and indirect costs [29], as presented in Table 1.

Table 1. Capital expenditure (CAPEX) and operating expenses (OPEX) in 2-tier Heterogeneous Cellular Network (HCN), also commonly referred to as HetNet, (HetNet).

Item	Macro BS (1 kW) [$]	Pico BS (250 mW) [$]
Equipment purchase (CAPEX)	50,000.00	5000.00
Equipment installation (CAPEX)	120,000.00	3000.00
Maintenance (OPEX)	2500.00	250.00
Site rental (OPEX)	10,000.00	1000.00
Backhaul rental (OPEX)	40,000.00	10,000.00
Energy consumption (OPEX)	3500.00	200.00
TOTAL	226,000.00	19,450.00

The linear regression model (of the form $y = ax^b + c$) for the sum C_{tot} of all costs [29] for a single BS with transmission power P_{BS}, in k-th tier, and within a limited time period:

$$\begin{gathered} C_{\text{tot}} = \sum_{k=1}^{N_T} \sum_{m=1}^{N_k} C_{\text{BS}_{k,m}} = \sum_{k=1}^{N_T} \sum_{m=1}^{N_k} \left(a \cdot P_{\text{BS}_{k,m}}^{b} + c \right) \\ N_T = 2,\ N_k \epsilon \{N_1, N_2\} \\ N_1 = \lambda_i \mathcal{A},\ N_2 = \lambda_j \mathcal{A} \\ \{a, b, c\} = \left\{ 8.807 \cdot 10^4, 0.305, -4.53 \cdot 10^4 \right\} \end{gathered} \tag{14}$$

was determined by means of the curve fitting feature of the MATLAB tool, providing the values of the coefficients a, b, and c in (14).

Here C_{tot} includes purchasing $k = 1, 2, \ldots, N_T$ macro-tier BSs and $m = 1, 2, \ldots, N_k$ small-tier BSs calculated from density of serving and candidate-serving tier BSs, electrical power costs, rental costs, and operation and maintenance costs. Most often, a ten-year period is adopted [30], whereas for any other, the coefficients a, b, and c would be different.

Note that indirect costs such as, e.g., the license, are not taken into account, as these are country- and time-dependent, but fixed within the observation period, which makes them not so relevant for *DE*.

Furthermore, network *DE* is defined as the ratio between the maximal data rate, i.e., network *SE* in bandwidth B, and the total cost of the network:

$$DE = \frac{B \cdot SE_{\text{TOT}}}{C_{\text{tot}}} \tag{15}$$

where (15) can be developed by taking into account (11), (12), (13), and (14) as:

$$DE = B \cdot \frac{\frac{\lambda_i}{\ln 2} \int_0^\infty \int_0^\infty \int_{\tau \cdot r_i}^\infty \frac{f_{\mathcal{R}_i}(r_i) \cdot f_{\mathcal{R}_j}(r_j) \cdot \mathcal{P}_i}{1+\gamma} d\gamma dr_i dr_j + \frac{\lambda_j}{\ln 2} \int_0^\infty \int_0^\infty \int_{\frac{r_i}{\tau}}^\infty \frac{f_{\mathcal{R}_i}(r_j) \cdot f_{\mathcal{R}_j}(r_i) \cdot \mathcal{P}_j}{1+\gamma} d\gamma dr_j dr_i}{\sum_{k=1}^{N_T} \sum_{m=1}^{N_k} \left(a \cdot P_{\text{BS}_{k,m}}^{b} + c \right)} \tag{16}$$

The above expression is valid for the scenario of network deployment which envisages two tiers ($N_T = 2$; pico and macro), each consisting of N_k BSs.

The relationship between the total deployment cost C_{tot} and the ratio $P_2^{\text{tx}} / P_1^{\text{tx}}$ of the relative transmit powers is visualized in Figure 3a, confirming that the benefits of spatial reuse of resources in a dense small-cell tier are significant. Comparing the scenarios of standalone pico and macro tiers emphasizes the strong potential of pico-tier deployments, especially for energy-efficient HetNets.

Moreover, according to (15), the trade-off between the total *DE* and *SE* is presented in Figure 3b, exhibiting three different cases, broken down by their θ values. The graph shows *SE-DE* improvement, while preserving the mean transmitter power within the range of a single BS power. In the region of lower *SE*, the expansion range bias has some impact on *SE-DE*, whereas in the region of high spectral density, it has low or no influence at all.

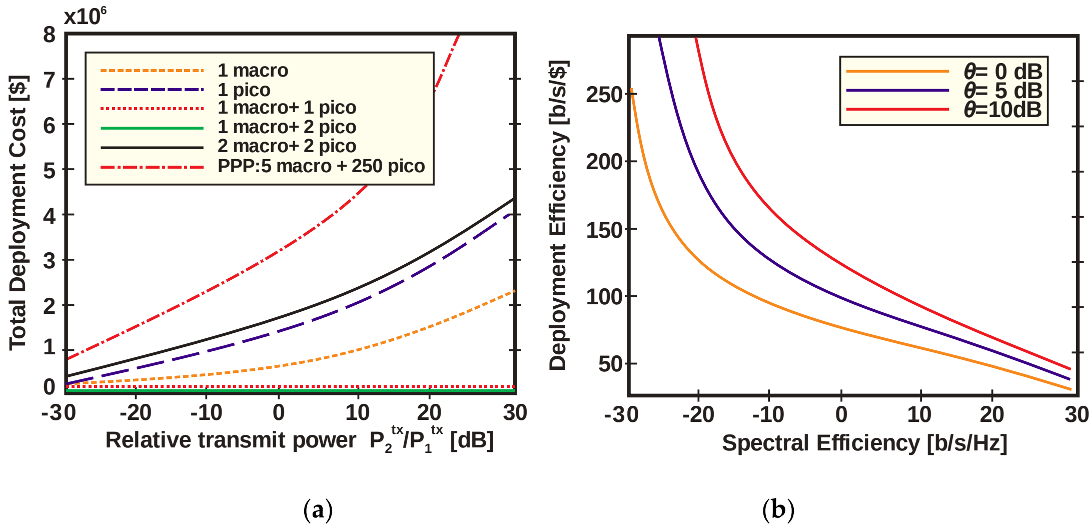

Figure 3. Total deployment costs and efficiency in the two-tier example: (**a**) deployment cost vs. transmit powers ratio: (**b**) deployment efficiency (*DE*) vs. *SE*.

3. Simulation Results

Aiming to validate the presented analytical model by the two above-described scenarios, the model is implemented by means of ns-3 network simulator (release 3.32 [31]), running in the Linux environment and enabling the testing of various scenarios and environments with appropriate LTE RF modules and extension options towards 5G [32].

The following set up data were used for simulation, with the values presented in Table 2:

- count of macro cell BSs: N_{macro},
- maximal output transmit power of the macro-cell BS: $P_{\text{cell\_macro}}$,
- maximal output transmit power of the small-cell BS: $P_{\text{cell\_small}}$,
- count of small-cell BSs: N_{small},
- population density per m^2: D,
- maximal distance between BSs in the macro cell: r_{macro},
- maximal distance between BSs in the small cell: r_{small},
- count of resource blocks in accordance to the standard for the 5 MHz channel: n_{RB} [1],
- center of the frequency operating band: f,
- LTE channel bandwidth: B.

Table 2. Network parameters used in ns-3 simulation.

Parameter	Value	Parameter	Value
N_{macro}	5	r_{macro}	500 m
$P_{\text{cell\_macro}}$	40 W	r_{small}	50 m
$P_{\text{cell\_small}}$	250 mW	n_{RB}	25
N_{small}	250	F	2.1 GHz
D	3.8×10^{-4}	B	5 MHz

We applied the Rayleigh statistical propagation model for the downlink channel [33], as it enables a drastically shorter program execution time than the computationally much more demanding three-dimensional 3GPP model [23].

The simulations were performed in five rounds, where the accuracy of the obtained results—*SINR* in particular, was improved by averaging, and the results were statistically processed in accordance with standard procedures for large data volumes [34].

In Table 3, the simulation results are presented and conform to the setup data from Table 2.

Table 3. Simulation results (after averaging).

SINR	*SE*[b/s/Hz]	*EE*[b/J]
11.98	17.28	0.53
11.06	15.96	1.04
10.55	15.22	1.65
9.86	14.22	3.09
9.45	13.63	4.45
9.16	13.22	5.75

Finally, in order to estimate DE for the two considered scenarios, we used (15) taking simulation results to calculate C_{TOT}, and (13) for SE_{TOT}.

Accordingly, the diagrams in Figure 4a–c represent SE, EE, and DE, respectively, obtained by the simulation of the two scenarios, using the parameters' values listed in Table 2.

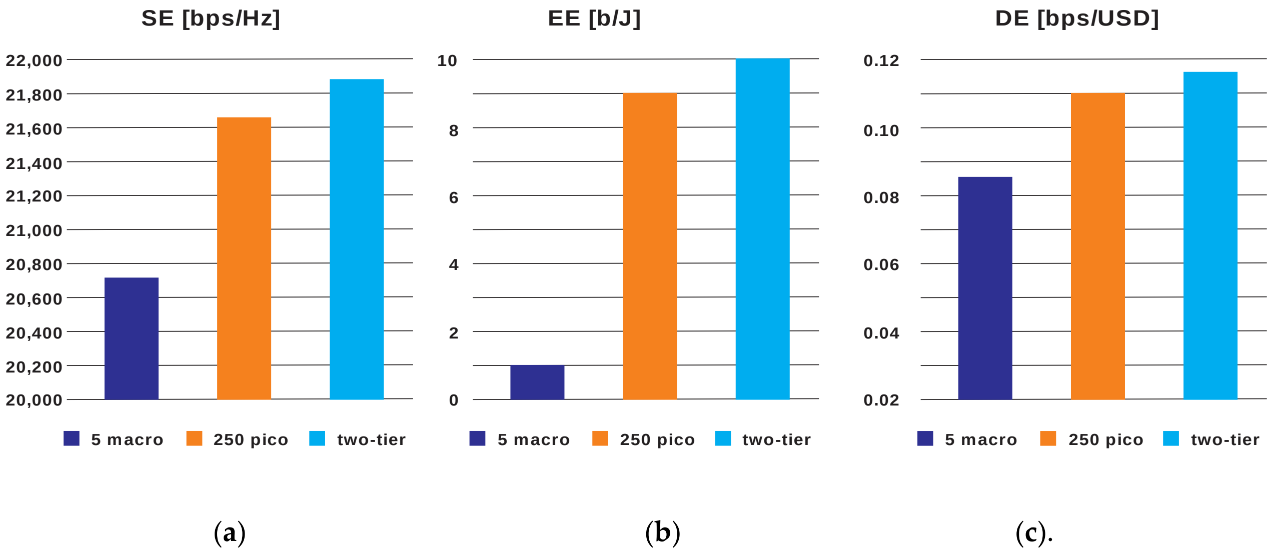

Figure 4. Simulation results: (**a**) SE, (**b**) EE, (**c**) DE.

4. Discussion

In each of the above three diagrams, it is noticeable that the two-tier scenario provided the most efficient network performance. Moreover, in all cases, better efficiencies were achieved with the small-cell scenario (250 pico BSs) than with macro cells (5 BSs) while preserving the same count and layout of users.

Furthermore, regarding the two-tier scenario, it is evident that, in addition to improved performance, it enables significant financial savings as well.

Moreover, considering different transmit power levels in the pico tier while keeping the macro-tier transmit power constant, SE shows a growing trend with respect to the ratio of transmit powers, Figure 5.

From the curves, it is evident that SE of the whole HetNet under consideration exhibits exponential growth with respect to the transmit power ratio, when small cells are introduced around a single macro cell. However, with only a single macro tier, it can be seen that SE does not change with transmit power ratio variation.

Consequently, the scenarios with a larger number of pico cells within the network inevitably lead to higher SE, which is in accordance with the expected values coming out of the analytical model presented in Section 2.

In summary, planning schemes affecting the efficiency of the overall heterogeneous micro/macro cell network, can adopt either BSs and UEs, being uniformly distributed in hexagonal geometrical structure, or their distribution that is based on stochastic geometry.

In this work, it is the latter one that we considered closer to reality than the former (deterministic) one.

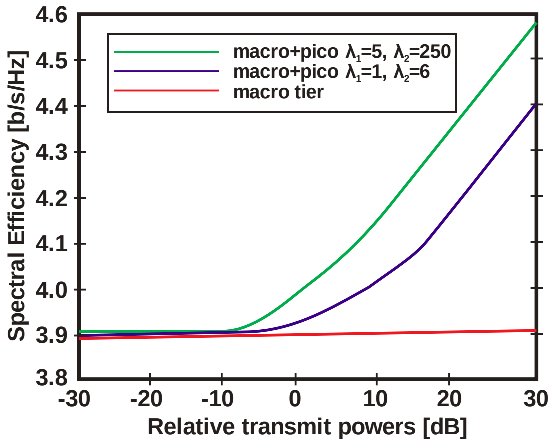

Figure 5. SE vs. transmit powers ratio.

Contributions of this work stem from the following:

Considering the locations of BSs and UEs to be PPPs, we introduced observing the OA small cells and not the small-cell CSG UEs. Having considered the CRE based selection of the serving BS, we derived analytical expressions for EE and SE for the two scenarios of interest.

Moreover, we extended the joint analysis of SE and EE with the cost-oriented DE, to exhibit the trade-offs among the three parameters.

Finally, our simulations have validated the significant benefits of cell planning according to the proposed model.

It is possible to further improve the analysis in terms of complexity and fairness, if the model is extended by various mechanisms of network resources' management [24], or by other PPP variants, such as Poisson Cluster Process (PCP) [35] or Matérn Hard-Core Process (MHCP) [27].

5. Conclusions

The overall HetNet efficiency has been analyzed by means of stochastic geometry modeling of UE and BS locations as mutually independent and homogeneous PPPs.

After the according model validation by means of the ns-3 network simulator, it came out that heterogeneous cellular networks to a large extent satisfy customer requirements for high spectral, energy, and deployment efficiency.

The analysis and simulation results imply that the introduction of small cells in heterogeneous networks with any chosen distribution of base stations has a major positive impact on energy and SE, as well as on deployment cost reduction.

Hence, reducing distances between BSs and UEs in state-of-the–art mobile networks—LTE and LTE-A, in particular—enables rationalizing and redistributing signal coverage towards areas of increased traffic demand and is definitely a very good strategy, which needs to be complemented with a number of other consideration factors such as: RF interference and impairments, traffic flow and frequency resources (bandwidth and channel allocation), whose management has to ensure the projected QoS level, complexity reduction, and fairness.

Author Contributions: Conceptualization, J.M., and V.L.; methodology, J.M. and V.L.; software, J.M.; validation, J.M., V.L., and A.L.; formal analysis, J.M. and A.L.; investigation, J.M.; resources, J.M. and A.L.; data curation, J.M.; writing—original draft preparation, J.M; writing—review and editing, A.L. and V.L.; visualization, J.M.; supervision, A.L.; project administration, A.L.; funding acquisition, J.M. All authors have read and agreed to the published version of the manuscript.

Funding: This research received no external funding.

Data Availability Statement: No new data were created or analyzed in this study. Data sharing is not applicable to this article.

Conflicts of Interest: The authors declare no conflict of interest. The funders had no role in the design of the study; in the collection, analyses, or interpretation of data; in the writing of the manuscript, or in the decision to publish the results.

References

1. Parkvall, S.; Dahlman, E.; Furuskar, A.; Jading, Y.; Olsson, M.; Wanstedt, S.; Zangi, K. LTE-advanced-evolving LTE towards IMT-advanced. In Proceedings of the 2008 IEEE 68th Vehicular Technology Conference, Calgary, AB, Canada, 21–24 September 2008; pp. 1–5.
2. Slamnik, N.; Okic, A.; Musovic, J. Conceptual radio resource management approach LTE heterogeneous networks using small cells number variation. In Proceedings of the 2016 XI International Symposium on Telecommunications (BIHTEL), Sarajevo, Bosnia and Herzegovina, 24–26 October 2016; pp. 1–5.
3. Slamnik, N.; Musovic, J.; Okic, A.; Tankovic, F.; Krijestorac, I. An approach to analysis of heterogeneous networks' efficiency. In Proceedings of the 2017 XXVI International Conference on Information, Communication and Automation Technologies (ICAT), Sarajevo, Bosnia and Herzegovina, 26–28 October 2017; pp. 1–5.
4. Bousia, A.; Kartsakli, E.; Antonopoulos, A.; Alonso, L.; Verikoukis, C. Energy Efficient Schemes for Base Station Management 4G Broadband Systems. In *Broadband Wireless Access Networks for 4G: Theory, Application, and Experimentation*; IGI Global: Hershey, PA, USA, 2014; pp. 100–120.
5. Imran, M.A.; Alonso-Rubio, J.; Auer, G.; Boldi, M.; Braglia, M.; Fazekas, P.; Ferling, D.; Fehske, A.; Frenger, P.; Gupta, R.; et al. Most suitable efficiency metrics and utility functions. *Earth Proj. Rep.* **2011**, 1–89, Deliverable D2.4.
6. ETSI TS 102 706 Standard, Environmental Engineering (EE) Measurement Method for Energy Efficiency of Wireless Access Network Equipment, V1.2.1. 2011. Available online: https://etsi.org (accessed on 30 January 2021).
7. ETSI TR 103 117, Environmental Engineering (EE); Principles for Mobile Network Level Energy Efficiency, v1.1.1. 2012. Available online: https://etsi.org (accessed on 30 January 2021).
8. Mukherjee, S. *Analytical Modeling of Heterogeneous Cellular Networks*; Cambridge University Press: Cambridge, UK, 2014; ISBN 978-1-107-05094-5.
9. Andrews, J.G.; Baccelli, F.; Ganti, R.K. A tractable approach to coverage and rate cellular networks. *IEEE Trans. Commun.* **2011**, *59*, 3122–3134. [CrossRef]
10. Baccelli, F.; Klein, M.; Lebourges, M.; Zuyev, S. Stochastic geometry and architecture of communication networks. *Telecommun. Syst.* **1997**, *7*, 209–227. [CrossRef]
11. Baccelli, F.; Błaszczyszyn, B. On a coverage process ranging from the Boolean model to the Poisson-Voronoi tessellation with applications to wireless communications. *Adv. Appl. Probab.* **2001**, *33*, 293–323. [CrossRef]
12. ElSawy, H.; Hossain, E.; Haenggi, M. Stochastic geometry for modeling, analysis, and design of multi-tier and cognitive cellular wireless networks: A survey. *IEEE Commun. Surv. Tutor.* **2013**, *15*, 996–1019. [CrossRef]
13. Brown, T. Cellular performance bounds via shotgun cellular systems. *IEEE J. Sel. Areas Commun.* **2000**, *18*, 2443–2455. [CrossRef]
14. Dhillon, H.S.; Ganti, R.K.; Baccelli, F.; Andrews, J.G. Modeling and Analysis of K-Tier Downlink Heterogeneous Cellular Networks. *IEEE J. Sel. Areas Commun.* **2012**, *30*, 550–560. [CrossRef]
15. Dhillon, H.S.; Ganti, R.K.; Andrews, J.G. Load-Aware Modeling and Analysis of Heterogeneous Cellular Networks. *IEEE Trans. Wirel. Commun.* **2013**, *12*, 1666–1677. [CrossRef]
16. Mukherjee, S. Distribution of downlink SINR heterogeneous cellular networks. *IEEE J. Sel. Areas Commun.* **2012**, *30*, 575–585. [CrossRef]
17. Madhusudhanan, P.; Restrepo, J.G.; Liu, Y.; Brown, T.X.; Baker, K.R. Multi-tier network performance analysis using a shotgun cellular system. In Proceedings of the 2011 IEEE Global Telecommunications Conference-GLOBECOM 2011, Houston, TX, USA, 5–9 December 2011; pp. 1–6.
18. Heath, R.W.; Kountouris, M.; Bai, T. Modeling Heterogeneous Network Interference Using Poisson Point Processes. *IEEE Trans. Signal Process.* **2013**, *61*, 4114–4126. [CrossRef]
19. Madhusudhanan, P.; Li, X.; Liu, Y.; Brown, T.X. Stochastic geometric modeling and interference analysis for massive MIMO systems. In Proceedings of the 11th International Symposium and Workshops Networks (WiOpt), Tsukuba, Japan, 13–17 May 2013; pp. 15–22.
20. Dhillon, H.S.; Kountouris, M.; Andrews, J.G. Downlink MIMO HetNets: Modeling, Ordering Results and Performance Analysis. *IEEE Trans. Wirel. Commun.* **2013**, *12*, 5208–5222. [CrossRef]
21. Kountouris, M.; Pappas, N. HetNets and massive MIMO: Modeling, potential gains, and performance analysis. In Proceedings of the 2013 IEEE-APS Topical Conference on APWC, Torino, Italy, 9–13 September 2013; pp. 1319–1322.
22. Chen, Y.; Zhang, S.; Xu, S.; Li, G.Y. Fundamental trade-offs on green wireless networks. *IEEE Commun. Mag.* **2011**, *49*, 30–37. [CrossRef]

23. Ademaj, F.; Taranetz, M.; Rupp, M. 3GPP 3D MIMO channel model: A holistic implementation guideline for open source simulation tools. *EURASIP J. Wirel. Commun. Netw.* **2016**, *55*, 1–4. [CrossRef]
24. Lee, Y.L.; Chuah, T.C.; Loo, J.; Vinel, A. Recent Advances in Radio Resource Management for Heterogeneous LTE/LTE-A Networks. *IEEE Commun. Surv. Tutor.* **2014**, *16*, 2142–2180. [CrossRef]
25. Badic, B.; O'Farrrell, T.; Loskot, P.; He, J. Energy efficient radio access architectures for green radio: Large versus small cell size deployment. In Proceedings of the IEEE 70th VTC Fall, Anchorage, AK, USA, 20–23 September 2009; pp. 1–5.
26. Demirtaş, M.; Soysal, A. Nonoverlay Heterogeneous Network Planning for Energy Efficiency. *Wirel. Commun. Mob. Comput.* **2017**, *2017*, 6519709. [CrossRef]
27. Yang, J.; Pan, Z.; Guo, L. Coverage and Energy Efficiency Analysis for Two-Tier Heterogeneous Cellular Networks Based on Matérn Hard-Core Process. *Future Internet* **2019**, *12*, 1. [CrossRef]
28. Blaszczyszyn, B.; Karray, M.K.; Keeler, H.P. Wireless Networks Appear Poissonian Due to Strong Shadowing. *IEEE Trans. Wirel. Commun.* **2015**, *14*, 4379–4390. [CrossRef]
29. Johansson, K.; Zander, J.; Furuskar, A. Modelling the cost of heterogeneous wireless access networks. *Int. J. Mob. Netw. Des. Innov.* **2007**, *2*, 58. [CrossRef]
30. Nikolikj, V.; Janevski, T. Applicable cost modeling of LTE-Advanced and IEEE 802.11 ac based heterogeneous wireless access networks. In Proceedings of the 10th Advanced International Conference on Telecommunications AICT, Paris, France, 20–24 July 2014.
31. Ns-3 User Documentation. Available online: http://www.nsnam.org/tutorials.html (accessed on 30 January 2021).
32. Wei, Y.; Gong, Y.; Li, Q.; Song, M.; Wang, X. Energy Efficient Resource Allocation Approach for Renewable Energy Powered Heterogeneous Cellular Networks. *Comput. Mater. Contin.* **2020**, *64*, 501–514. [CrossRef]
33. Crane, R.K. *Propagation Handbook for Wireless Communication System Design*; CRC Press: Boca Raton, FL, USA, 2003; pp. 74–88.
34. Wang, J.; Yang, Y.; Wang, T.; Sherratt, R.S.; Zhang, J. Big Data Service Architecture: A Survey. *J. Internet Technol.* **2020**, *21*, 393–405.
35. Saha, C.; Afshang, M.; Dhillon, H.S. 3GPP-Inspired HetNet Model Using Poisson Cluster Process: Sum-Product Functionals and Downlink Coverage. *IEEE Trans. Commun.* **2018**, *66*, 2219–2234. [CrossRef]